

## MONITORING OF THE MOVEMENTS OF A DEEP, SLOW, CLAYEY LANDSLIDE AND 3D INTERPRETATION

ROBERTO VASSALLO<sup>(\*)</sup>, ROSSELLA PAGLIUCA<sup>(\*)</sup> & CATERINA DI MAIO<sup>(\*)</sup>

<sup>(\*)</sup> University of Basilicata - School of Engineering - Via dell'Ateneo Lucano 10 - 85100 Potenza, Italy  
E-mail: roberto.vassallo@unibas.it - Tel. +390971205390

### ABSTRACT

The *Costa della Gaveta* landslide is an active, deep and very slow landslide which is being monitored and studied since 2004. Recently new boreholes have been carried out and inclinometer tubes have been installed to deepen the comprehension of the 3D geometry and kinematics. Localized displacement on a slip surface is confirmed to be the prevailing movement mechanism. Thanks to the long term monitoring, even the slow internal viscous deformations of the landslide body have been evaluated and interpreted. Soil discharge (i.e., the volume rate of soil crossing transversal sections) is confirmed to be constant in the track. This characterizing kinematic feature allows a first approximation prediction of the landslide behaviour on empirical basis.

To further improve the prediction of the landslide behaviour and the risk management of the area, a theoretical model has been constructed by a 3D finite element code. First results show the large difference in the safety factor between 2D and 3D analyses for the considered landslide. The influence of pore pressure distribution on the local safety factor is also analysed.

**KEY WORDS:** landslide, displacements, inclinometer, prediction, stability

### INTRODUCTION

The *Costa della Gaveta* landslide occurs close to the city of Potenza, Italy, in a structurally complex clay formation, locally known as Varicoloured Clays.

The landslide is from very to extremely slow. In fact, in the monitoring period, the displacement rates have always been in the order of one cm/year in the middle of the track, where only a few houses have been built in the last twenty years, and seem still unaffected by the slope movements. On the contrary, at the landslide head - which is the fastest zone - a house has recently been evacuated because it is threatened by the landslide and by a shallow earth-flow occurring in the main scarp. The landslide foot, which is the slowest part, with average rates in the order of a few mm/year, is crossed by a highway and by the national railway and several buildings arise on it.

With the exception of the head of the landslide, the rates of displacement are too low to vacate inhabitants or deviate roads and railway. In addition, the landslide is very deep and thus very difficult to stabilize. On the other hand, a deep understanding of the landslide, which permits to predict its behaviour, can contribute to minimize the associated risk.

In order to understand how and when the landslide movement can cause damage to houses and infrastructures, inclinometer tubes for both standard, periodical measurements and continuous data acquisition were installed since 2004 (Fig.1). GPS permanent and periodical stations were also installed. Piezometer measurements, *in situ* permeability tests and laboratory mechanical tests were carried out.

The maximum detected depth of the slip surface resulted of about 40 m. Displacement profiles

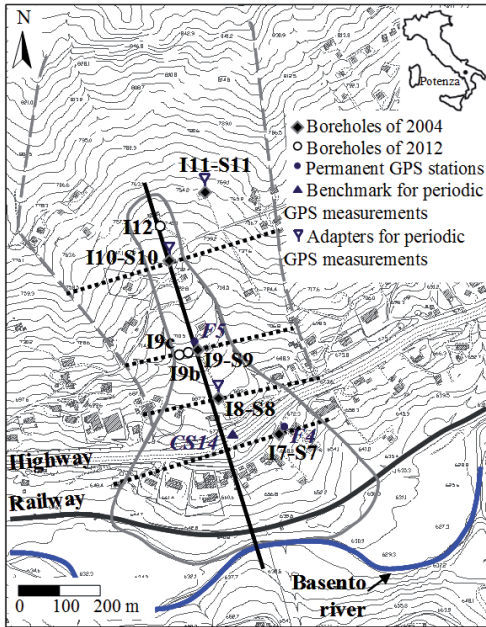


Fig. 1 - Landslide boundaries, inclinometers, piezometers, GPS stations, and considered longitudinal and transversal sections

obtained in the first years - mostly along the landslide median longitudinal section - were practically uniform in each inclinometer from the slip surface to the ground: sliding along the slip surface was thus considered the prevailing mechanism of displacement. Furthermore, in the observation period, the displacement rates were always noticeably decreasing from upslope to downslope. Under the hypothesis that displacements were uniform not only along the inclinometer vertical but in each entire transversal section of the track, DI MAIO *et alii* (2010) interpreted the decrease of displacement rate as an effect of the increase in the areas of transversal sections in the downslope direction, the resulting "soil discharge" (i.e., the volume of soil crossing transversal sections in the unit time) being practically constant.

In the first half of 2012 new boreholes have been carried out and inclinometer tubes have been installed to study the kinematics of a transversal section of the track. Based on previous and new data, this paper proposes a 3D empirical model of the landslide. The contribution of internal viscous deformations to ground displacements and soil discharge are also considered. Furthermore, a 3D finite element (FEM) theoretical model of the landslide has been imple-

specific gravity $G$	2.05 - 2.15
clay fraction $c.f.$	20 - 60 %
porosity $n$	33 - 42 %
degree of saturation $S$	95 - 100 %
plasticity index $PI$	20 - 55%
hydraulic conductivity ( <i>in situ</i> )	$10^{-9}$ - $10^{-10}$ m/s
hydraulic conductivity (laboratory)	$10^{-11}$ - $10^{-12}$ m/s
average peak friction angle $\phi$	$14^\circ$
average cohesion intercept $c'$	50 kPa
average residual friction angle $\phi_r$	$10^\circ$

Tab. 1 - Physical characteristics, index, hydraulic and mechanical properties of the finer part of the landslide material

mented with the aim of evaluating the stress-strain distribution within the landslide body and its variations induced by the possible triggering factors. The difference in the safety factor provided by a 2D and a 3D model is also analysed.

## SUBSOIL CHARACTERIZATION

The landslide occurs within the geological formation of the Varicoloured Clays (Upper Cretaceous - Oligocene), which is made up of a succession of chaotic, severely tectonized scaly clays and marly clays. The formation includes rock fragments or blocks or even strata of marly limestone, calcareous marl and calcarenite. The soil is markedly heterogeneous, similarly in the landslide body and in the stable soil underneath (DI MAIO *et alii*, 2010).

Tab. 1 reports the ranges of some physical characteristics of the finer, clayey matrix. Because of the diffuse presence of rock fragments, only a few undisturbed samples could be extracted from the boreholes indicated in Fig. 1. On these samples, the peak shear strength of the landslide material was evaluated by isotropically consolidated - undrained (CIU) triaxial tests. The residual strength was evaluated by direct shear tests on both the undisturbed and the reconstituted material. The details of the experimentation are reported in DI MAIO *et alii* (2010). The peak strength is characterized by average  $c' = 50$  kPa and  $\phi' = 14^\circ$ , while the residual strength is characterized by  $c' = 0$  and average  $\phi'_r$  of about  $10^\circ$ , as reported in Tab. 1. Thus, a noticeable drop of strength from peak to residual is observed. In the finite element analyses, the available strength on the slip surface will be hypoth-

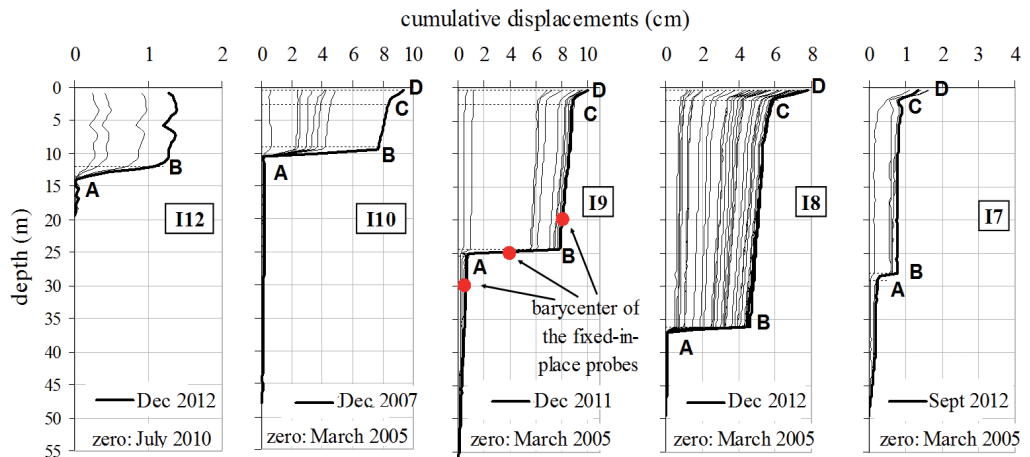


Fig. 2 - Cumulative displacement profiles of casings installed close to the axial longitudinal section

esized to be close to the residual, consistently with the observation that this active and ancient landslide underwent large displacements along a regular slip surface. Hence, if this hypothesis is correct, the shear strength within the landslide body is much higher than that on the slip surface. As reported by DI MAIO *et alii* (2010) and VASSALLO *et alii* (2012a-b) such feature is recognized in the literature as an important factor determining the style of displacements and justifying the prevailing contribution of sliding at the base.

Hydraulic conductivity was estimated *in situ* by carrying out falling head tests, and in laboratory by interpreting the consolidation curves of oedometer tests. The estimated conductivity values, reported in Tab. 1, are very low and this strongly influences the landslide response to rainfall (VALLARIO, 2012).

### INCLINOMETER MEASUREMENTS

Five inclinometer casings, up to 50 m deep, were installed in the landslide at the end of 2004, in the positions indicated by Fig. 1. In 2006, a GPS network of permanent and non-permanent stations was installed for the evaluation of surface displacements. In the observation period, a good consistency was found between inclinometer and GPS measurements (CALCATERRA *et alii*, 2012). Other inclinometers were installed recently, in the first half of 2012.

A selection of the many measurements carried out from 2005 to today is reported in Fig. 2 in terms of inclinometer cumulative displacement profiles. Casing I10 was found out of use in August 2008. Casing I9 was used for different kinds of measurements. In July

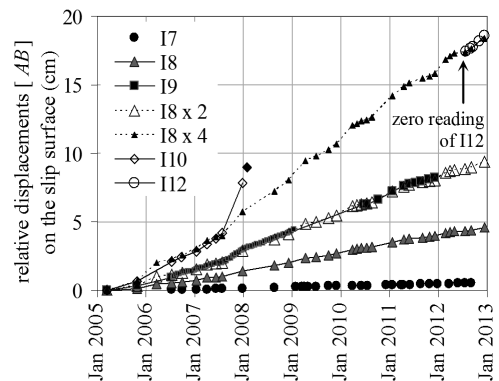


Fig. 3 - Deep displacements against time

2006, when the slip surface in it had been clearly detected, three fixed-in-place probes were installed, one in correspondence to the slip surface and the other two in the landslide body and in the stable soil respectively (Fig. 2). In January 2009, the fixed-in-place probes went out of use. In July 2010, they were removed and inclinometer measurements were carried out by mobile probe again. A very good agreement was found between displacements measured in such different ways, as it is possible to appreciate from data of I9 reported in Fig. 3. At the beginning of 2012, the tube was found pinched off in correspondence to the slip surface, so, that of December 2011 is the last measurement carried out beneath the slip surface. Inclinometers I11, I18 and I17 are still in full use today.

Figure 2 shows that three components of displacement can be clearly distinguished and analysed in each inclinometer profile: AB, corresponding to slid-

ing along the slip surface, BC and CD, resultants of internal deformations of the landslide body, which are more pronounced in the upper 2-2.5 m thick soil layer, consisting of remoulded organic soil characterized by poor mechanical properties (DI MAIO *et alii*, 2013).

The sliding component AB largely prevails on the others, also in the inclinometer I12 recently installed, and thus gives the character of substantial uniformity to the profiles.

Figure 3, which reports deep displacements on the slip surface against time, shows that the AB components are strongly correlated to each other in the whole observation period. In particular, it can be observed that displacements in I9 are very close to those of I8 multiplied by 2. Furthermore, displacements of I8 multiplied by 4 are in good agreement with both those of I10 and those of I12. It can be said that, with the exception of the period of apparent acceleration that led I10 to failure, deep displacements of any two inclinometer casings keep an almost constant ratio (DI MAIO *et alii*, 2013). This is actually one of the first considerations on the basis of which DI MAIO *et alii* (2010) hypothesized the constancy of the soil discharge.

The displacement rates, which correspond to the slope of the curves in Fig. 3, range from 2 - 3 cm/year in the upper portion of the track to about 1 mm/year in the accumulation. Actually, the extremely slow displacements measured in I7 have been considered realistic because of their regular evolution over 7 years, besides their clear azimuth trend.

It is worth noting that in the period 2006-2009 the landslide rarely came to a stop. This is shown by Fig. 4, where the displacement rate in I9 in that period is computed from the measurements of the central fixed-in-place probe, installed in correspondence to the slip surface. The rate went rarely down to zero, and always attained very small values, with minimums and maxi-

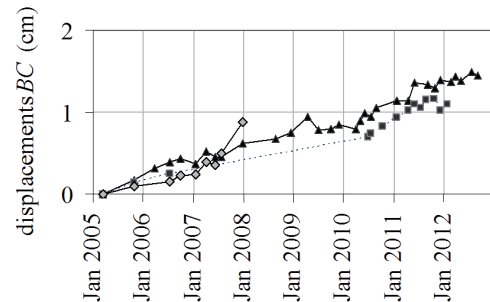


Fig. 5 - Displacements against time: BC and CD components (defined in Fig. 3)

mums differing of less than an order of magnitude. So, it seems possible to refer to an average almost constant displacement rate which, in the case of I9, is about 1 cm/year.

As for the trends of the BC and CD components, reported in Fig. 5, one can observe their low values and an average continuous increase in time. DI MAIO *et alii* (2013) propose an interpretation of their general trends based on Bingham's rheological model and on the results of long term laboratory shear creep tests.

At the beginning of 2012 two new inclinometer tubes, I9b and I9c, have been installed in the transversal section through I9, in the position indicated in Fig. 1. Because of the extremely slow rate of movements, at the moment, these two inclinometers provide only qualitative information susceptible to variations. However, first results seem consistent with the measurements of I9 in terms of slip surface position, as will be shown in the next section. Another interesting feature is that in these lateral boreholes internal deformations seem more significant than those of the median longitudinal section and contribute to a noticeable percentage of total displacements. DI MAIO *et alii* (2013) report the water content ( $w$ ) profiles of I9b and I9c showing that in both boreholes the slip surface is close

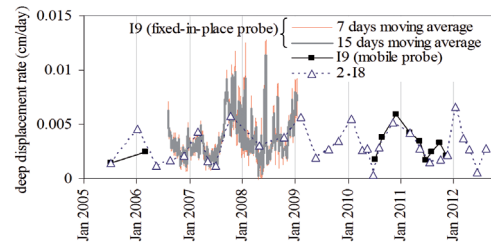
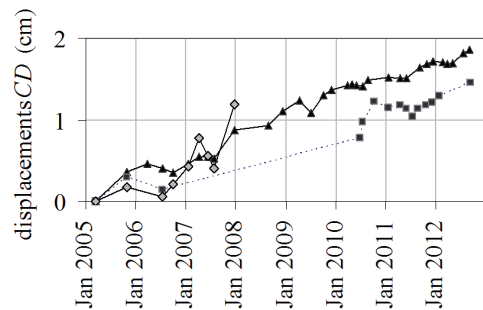


Fig. 4 - Displacement rate on the shear surface in I9 and I8 against time, obtained from fixed-in-place probe and mobile probe measurements



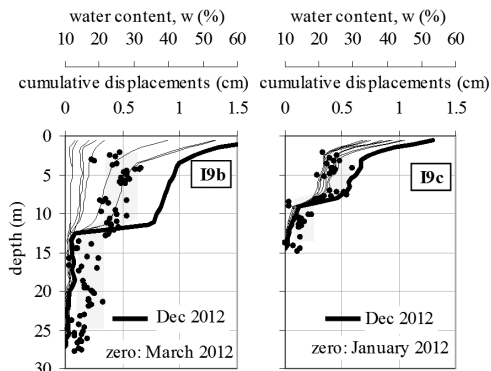


Fig. 6 - Cumulative displacement profiles and water content profiles of I9b and I9c

to the boundary between less consistent ( $w=25\%$ ) and more consistent ( $w=15\%$ ) soil, as shown in Fig. 6, where displacement profiles and water content data are compared. On the contrary, in I9 the slip surface goes through the more consistent material. The different water content is thus considered a possible explanation of the different viscous deformations.

## GEOMETRICAL FEATURES

The landslide is characterized by a large well-defined fan-shaped foot, a track with regular flanks and a wide depletion zone (Fig. 1). The main geometrical features of the landslide were described by DI MAIO *et alii* (2010). In particular, the trace of the slip surface in the median longitudinal section was drawn on the basis of the inclinometer profiles (Fig. 7a). The landslide detected depth increases from about 10 m in inclinometer I10 to 38 m in inclinometer I8. This latter can be considered at the transition from the track to the accumulation, which extends down to the Basento river and is partly subjected to its erosion (VASSALLO *et alii*, 2012a). The geometry of some cross sections of the landslide body (Fig. 7b) were drawn by DI MAIO *et alii* (2010) on the basis of the inclinometer profiles and of the elaboration of geometrical characteristics of the flanks of the track, which were considered as the outcropping portion of the slip surface. The resulting cross section areas were found strongly increasing in the downslope direction. This has been considered as a cause of the significant decrease in the average displacement rate from I10 to I7 clearly shown by the data in Fig. 3.

The inclinometers recently installed add further information about the landslide geometry and kinematics. Inclinometer I12 is located at the landslide

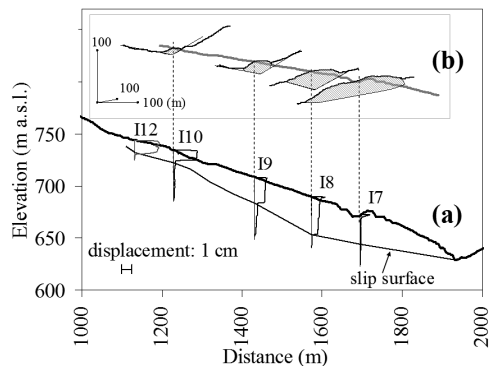


Fig. 7 - Slip surface in the longitudinal median section (a) and in some transversal sections (b)

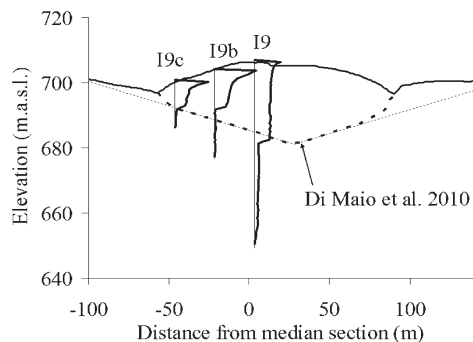


Fig. 8 - Displacement profiles of inclinometers I9, I9b and I9c and comparison with the slip surface hypothesized by Di MAIO *et alii* (2010)

head. Although the details of the landslide geometry in this zone are still under study, the depth of failure has been clearly detected (Fig. 7a).

Measurements in lateral inclinometers I9b and I9c contribute to investigate the geometry of a transversal section, as shown by Fig. 8, where they are compared to the data of the central inclinometer I9. The measurements in I9c indicate a position of the slip surface very close to that hypothesized by DI MAIO *et alii* (2010), whereas, in I9b, the slip surface is detected 3 m above the hypothesized depth. So, the geometrical reconstruction proposed by DI MAIO *et alii* (2010) for the three cross sections through the inclinometers I8, I9 and I10 can be reasonably extended to the whole track. Figure 9 reports a simplified scheme of the slip surface both in the landslide track and in the accumulation, which takes into account experimental data, theoretical elaborations and simplification requirements of numerical calculation. Two planes, *a* and *b*, were used to describe the slip surface in the track. They

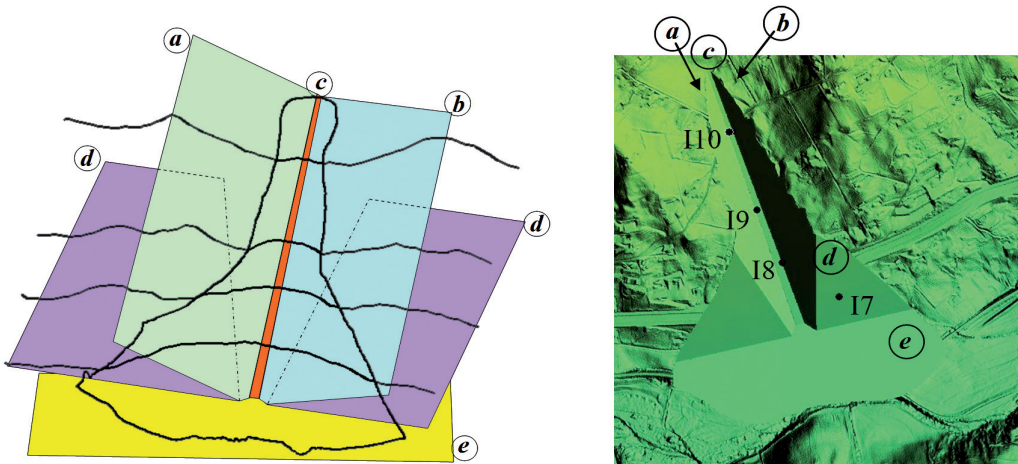


Fig. 9 - Three-dimensional scheme of the slip surface, consisting of: two planes (a and b) in the track area; a third plane (c) used to smooth off the angle formed by the first two; a transition plane (d); the floodplain (e)

are the best fitting planes through the lateral channels and through the slip surface detected by inclinometers. Plane *c* smooths off the angle formed by the first two in order to avoid numerical problems in the FEM model. Plane *d*, with an inclination greater than that of the hill slope, describes the transition to the river floodplain. The existence of such plane emerges from the analysis of the ground surface topography. Its geological origin is currently under study. Plane *e* is the best fitting plane of the river bank. Such scheme was used for constructing the slip surface in the 3D finite element model. Fig. 9 also shows the simplified slip surface inserted into the DTM of the slope.

### 3D INTERPRETATION OF EXPERIMENTAL DATA

The reconstruction of the 3D geometry of the landslide and the description of its fundamental kinematic features can be the basis of a prediction model. In fact, under the hypothesis of: a) constant soil discharge through the different transversal sections of the track, and b) soil discharge independent of time, predictions are possible, in the absence of exceptional events such as earthquakes or extreme rainfall. In fact, average displacement rates and then displacements over a generic time interval can be calculated.

As for the assumption of constant soil discharge through different transversal sections, Di MAIO *et alii* (2013) evaluate the soil volume crossing the transversal sections against time including the creep effect. On the basis of measured inclinometer profiles I9, I9b and

I9c and of the relative position of these boreholes in the cross section, they hypothesized uniform displacements at each given elevation for any cross section of the track (Fig. 10). Just for the upper 2 m thick weathered soil, where the shear creep rate is higher, an additional contribution, uniform at each given depth from the ground surface, was considered. The soil volumes relative to the transversal section through I8 are slightly higher than those relative to the sections through I9 and I10 (Fig. 10). The volumes almost coincide if the cross section through I8 is multiplied by 0.75. So, assuming a constant soil discharge is confirmed to be more than reasonable.

It is worth noting that, thus far, the volumes calculated including the creep effect are just slightly higher than those which would be estimated by considering the displacements uniform in each transversal section. Nevertheless, under unchanged conditions, such difference is going to increase as years go by.

In the case of the cross section through I7, the displacements are still very small. In I7 it is not possible to distinguish the internal deformations, with exception of those of the upper 2.5 m thick superficial layer, and, *a fortiori*, it is not possible to hypothesize a distribution of internal deformations in the section. The sliding component does not seem uniform in the section, as reported in detail by Di MAIO *et alii* (2010). The volumes through I7 reported in Fig. 10 were thus calculated in two different ways, as schematized in Fig. 10 and reported by Di MAIO *et alii* (2013).

From Fig. 10, an average soil discharge in the

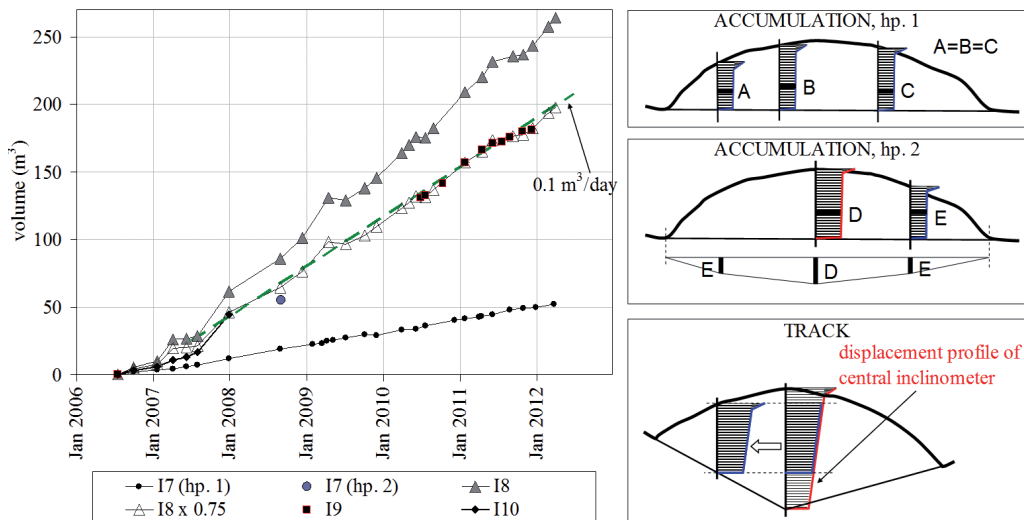


Fig. 10 - Volume of soil crossing the transversal sections in the monitoring period

track can be evaluated:  $Q \approx 0.1 \text{ m}^3/\text{day}$ . If our interpretation is correct, then it is possible to use data obtained in a few instrumented zones to estimate the displacements in any other zone of the landslide. This is shown by Fig. 11 which reports the transversal section areas  $A$  along the longitudinal axis and the average displacement rate ( $v=Q/A$ ) in the transversal sections. Actually, sliding largely prevails on creep internal deformations, so the real rates in any point of each transversal section are very close to the average values reported in the figure. Under the hypothesis that such rates keep constant over a certain number of years, the displacements can be calculated and thus the expected damage can be evaluated (MANSOUR *et alii*, 2011).

**3D FEM MODEL**

A 3D finite element model has been implemented by the Plaxis3D code. A mesh including about 112,000 10-noded tetrahedral elements has been adopted (Fig. 12a). The ground surface is described by a grid with a maximum thickness of 10 m. The landslide body is saturated even above the water table (with unit weight  $\gamma_{\text{sat}} = 21 \text{ kN/m}^3$ ), homogeneous, isotropic and characterized by an elastic-perfectly plastic behaviour with a Young modulus  $E' = 50 \text{ MPa}$  and a Poisson's ratio  $\nu' = 0.40$ . The cohesion and friction angle of the soil are respectively  $c' = 50 \text{ kPa}$  and  $\phi' = 14^\circ$ , as from laboratory tests. The slip surface reported in Fig. 9 has been simulated with interface elements characterised by a perfectly plastic behav-

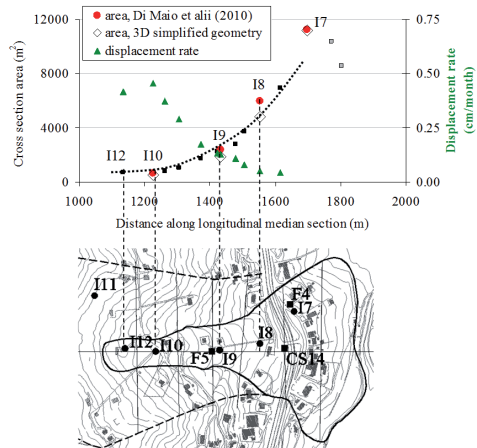


Fig. 11 - Estimate of average displacement rate in the transversal sections. Data relative to I12 are still preliminary

our with zero cohesion and by various friction angle values for parametric calculations. The code allows to define the pore pressure distribution by imposing a phreatic surface; the piezometric head is considered constant along each vertical. In the following example, three different positions of the phreatic surface are considered, one coincident with the ground surface and the others at 2 and 4 meters below the ground surface, respectively.

The stress distribution on the slip surface is one of the possible outputs of the code. For any considered case, the safety factor SF was calculated following STIANSON *et alii* (2011):

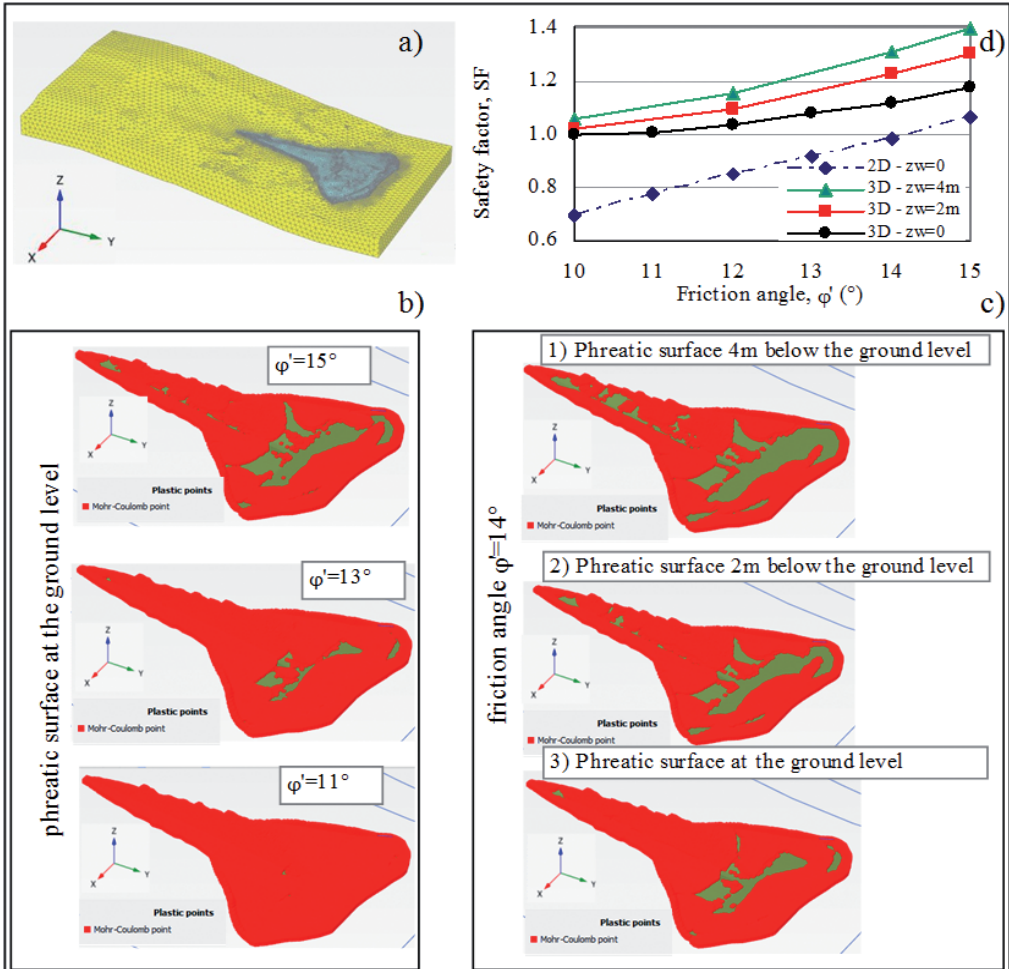


Fig. 12 - Plaxis 3D results. a) 3D mesh; b) distribution of plastic points obtained by fixing the phreatic surface at the ground level and considering three different friction angle values on the slip surface; c) distribution of plastic points for  $\phi'_r = 14^\circ$  and for three different positions of the phreatic surface; d) safety factor against friction angle (the 2D calculation is relative to a phreatic surface at the ground level, 3D calculations refer to a phreatic surface with depth  $zw$  of 4m, 2m and 0 from the ground surface)

$$SF = \frac{\sum \tau_{max,i} \cdot A_i}{\sum \tau_i \cdot A_i}$$

where the sums are extended to all the triangular elements of area  $A_i$  constituting the slip surface while  $\tau_{max,i}$  and  $\tau_i$  are the available shear strength and the acting shear stress respectively.

Figure 12 reports, for several considered cases, the distribution of plastic points on the slip surface. In particular, Fig. 12b reports the results obtained by fixing the phreatic surface at the ground level and considering three different friction angle values on the slip surface. It is interesting to observe that even for  $\phi'=15^\circ$  the material in the track and in the lowermost portion

of the accumulation are at failure, independently from each other. This seems in agreement with the physical observation of a local instability caused by river erosion at the toe (VASSALLO *et alii*, 2012a). Figure 12c reports the results obtained by fixing the friction angle value to  $14^\circ$  and considering three different depths of the phreatic surface. This figure shows how the safety factor would evolve in response to seasonal changes in boundary conditions, under the hypothesis of an instantaneous response at any depth. Actually, due to the low hydraulic conductivity, the phenomenon is strongly time-dependent. VALLARIO (2012) carried out pore pressure calculations in several longitudinal sections

of the considered landslide, from the median axis to the lateral channel. The Author found that in the median section, where the slip surface reaches a depth of 38 m, the historical rainfall series does not cause significant pore pressure changes. Closer to the lateral channels, where the slip surface is less deep, rain effects become more pronounced and the safety factor exhibits appreciable seasonal variations. The results reported in Fig. 12c are thus only a first step of the analysis that allows to verify if the model works correctly. The study of the time-dependent phenomenon is one of the real goals of our research.

The safety factor computed for the above cases and for other similar cases are reported in Fig. 12d. For comparison, the safety factor evaluated by a 2D analysis is also shown. This latter safety factor was obtained by limit equilibrium analyses carried out by the Slope/W code of the Geostudio suite on the longitudinal medium section, with phreatic surface coincident with the ground surface. Under equal conditions, in the friction angle range in which the comparison is possible (i.e., for  $SF > 1$ ) the global safety factors calculated by the 3D analysis are higher than those of the 2D analysis. Of course, the advantage of a 3D analysis is the possibility of studying the local conditions of stability, if the model is verified to be reliable. Such verification is currently being carried out by comparison of theoretical and experimental stress distributions.

## REFERENCES

- CALCATERRA S., CESI C., DI MAIO C., GAMBINO P., MERLI K., VALLARIO M. & VASSALLO R. (2012) - *Surface displacements of two landslides evaluated by GPS and inclinometer systems: a case study in Southern Apennines, Italy*. Natural Hazards, **61**: 257-266.
- DI MAIO C., VASSALLO R. & VALLARIO M. (2013) - *Plastic and viscous shear displacements of a deep and very slow landslide in stiff clay formation*. Engineering Geology, **162**: 53-66.
- DI MAIO C., VASSALLO R., VALLARIO M., PASCALE S. & SDAO F. (2010) - *Structure and kinematics of a landslide in a complex clayey formation of the Italian Southern Apennines*. Engineering Geology, **116**: 311-322.
- FELL R., COROMINAS J., BONNARD C., CASCINI L., LEROI E. & SAVANE W.Z. (2008) - *Guidelines for landslide susceptibility, hazard and risk zoning for land-use planning*. Engineering Geology, **102**: 99-111.
- MANSOUR M.F., MORGENSTERN N.R. & MARTIN C.D. (2011) - *Expected damage from displacement of slow-moving slides*. Landslides, **8** (1): 117-131.
- STIANSON J.R., FREDLUND D.G & CHAN D. (2012) - *Three-dimensional slope stability based on stresses from a stress-deformation analysis*. Canadian Geotechnical Journal, **48**: 891-904.
- VALLARIO M. (2012) - *Kinematics of two landslides in Varicoloured Clays and analysis of possible triggering factors*. Ph.D. Thesis (in Italian), University of Basilicata, Potenza, Italy.
- VASSALLO R., DI MAIO C., COMEGNA L. & PICARELLI L. (2012a) - *Some considerations on the mechanics of a large earthslide in stiff clays*. Proc. XI Int. Symp. on Landslides, Banff, Canada, **1**: 963-968.
- VASSALLO R., DI MAIO C., VALLARIO M. (2012b) - *A possible mechanism of movement of an ancient clayey landslide*. Proc. II World Landslide Forum, Rome, Italy, **2**: 273-279.

## CONCLUDING REMARKS

On the basis of a long term monitoring and of a recent integrative investigation, the geometry and the kinematics of the *Costa della Gaveta* landslide have been reconstructed. In the observation period, the displacement rate variations have been negligible. So, under the hypothesis of constant soil discharge through the different transversal sections of the track, and of soil discharge independent of time, displacement predictions on pure empirical basis are possible, obviously in the absence of exceptional events such as earthquakes or extreme rainfall.

A further improvement in the comprehension and prediction of the landslide behaviour can be achieved through a robust theoretical model. In the case under consideration, a conceptually satisfying model requires considering the 3D conditions. In fact, first results obtained by Plaxis3D show the large difference in the safety factor between 2D and 3D analyses under hydraulic steady state conditions. Such difference reasonably increases when the transient processes induced by the historical rainfall series are considered. The study of these transient processes is one of the next goals of our study.

## ACKNOWLEDGEMENTS

The Authors would like to thank Mr M. Belvedere who carried out the in situ measurements from 2011 on.

